

Morphology and multigene phylogeny reveal two novel species and three new records of Polypores in Swat, Pakistan

Shahid Hussain^{1*}, Mohammad Nisar¹, Young Woon Lim², Yoonhee Cho², Hassan Sher³, Tour Jan¹ and Waqas Ahmad³

¹ Department of Botany, University of Malakand, Chakdara Dir Lower-18800, Khyber Pakhtunkhwa, Pakistan

² School of Biological Sciences and Institute of Microbiology, Seoul National University, Gwanak-ro, Gwanak-gu, Seoul 08826, South Korea

³ Center for Plant Sciences and Biodiversity, Ala Abad Charbagh, Swat, Khyber Pakhtunkhwa 19120, Pakistan

* Corresponding author, E-mail: shahid_sattar84@yahoo.com

Abstract

Polypores, as wood-rotting fungi, play a vital ecological role in breaking down the wood substrate, releasing crucial nutrients into the soil, shaping the carbon dynamics, and contributing to the overall health of the forest ecosystem. Despite their significance, the fungal diversity in the Hindu Kush region remains inadequately explored. This study collected specimens from district Swat, Khyber Pakhtunkhwa Province, Pakistan, a part of the Hindu Kush region. After a rigorous examination of the collected specimens for the morphoanatomical characteristics, the concatenated sequence dataset (ITS + nrLSU) derived from generated sequences along with valid and published reference sequences was subjected to phylogenetic analyses using different methods: maximum parsimony, maximum likelihood, and Bayesian analyses. The study revealed two new species from the country, belonging to two polypores families i.e., *Climacocystaceae* and *Fomitopsidaceae*. Furthermore, the analysis confirmed the identification of *Daedalea dickinsii* Yasuda, *Neoantrodia serialis* (Fr.) Audet, and *Rhodofomes roseus* (Alb. & Schwein.) Kotl. & Pouzar as a new addition to the polypore inventory of Pakistan. These species received phylogenetic support and were proven to have corresponding morphological characteristics concerning pertinent original descriptions. The inclusion of these new wood-inhabiting fungi in the country's mycofloral list expands our understanding of fungal diversity, and distribution patterns, and contributes to global fungal biodiversity.

Citation: Hussain S, Nisar M, Lim YW, Cho Y, Sher H, et al. 2024. Morphology and multigene phylogeny reveal two novel species and three new records of Polypores in Swat, Pakistan. *Studies in Fungi* 9: e004 <https://doi.org/10.48130/sif-0024-0005>

Introduction

Polyporales Gäum represents a taxonomically diverse group of fungi that have received much scientific attention due to their fundamental ecological functions in the forest ecosystem. Because of their lignicolous habit, they are associated with different types of forest woods and cause different types of rot in both living and dead tree species^[1]. They are responsible for the disintegration of wood components and help humification and mineralization processes^[2]. Based on phylogenetic analyses of nrRNA genes and other protein-coding genetic markers, 29 lineages at the family level have been revealed in this group^[3]. One important family found in the Antrodia clade of Polyporales is *Fomitopsidaceae* Jülich 1981, which consists of brown-rotting genera, such as *Antrodia* P. Karst., *Daedalea* Pers., and *Fomitopsis* P. Karst.^[4–6]. Recently, many authors have undertaken consistent taxonomic revisions within Polyporales. For instance, Binder et al.^[7] and Justo et al.^[8] specified that the genera *Climacocystis* Kotl. & Pouzar and *Diplomitoporus* Domański exhibit an independent status in the phylogenetic analyses, and their familial placement remained uncertain^[9]. In a subsequent study by Liu et al. a new family named *Climacocystaceae* was proposed to accommodate these genera^[3].

Climacocystis Kotl. & Pouzar was introduced as a monotypic genus comprising only the type species *Climacocystis borealis* (Fr.) Kotl. & Pouzar^[10]. This genus belongs to the residual poroid clade and shares a close phylogenetic relationship with

Diplomitoporus Domański, *Physisporinus* P. Karst., and *Steccherinum* Gray^[11]. The genus is characterized by annual, pileate basidiocarps, a monomitic hyphal system with clamped generative hyphae, thick-walled ventricose cystidia, thin-walled, broadly ellipsoid basidiospores that do not react to Melzer's reagent. *Climacocystis* is rarely distributed in the northern hemisphere and is known to cause white rot in gymnosperms^[7,12–15]. In 2014, *Climacocystis montana* B.K. Cui & J. Song was added to the genus as a new species from high-altitude temperate forests in China^[11].

Among the brown-rotting polypores, *Fomitopsis* P. Karst. sensu lato (s.l.) is the largest genus in terms of species diversity. The genus is characterized by annual to perennial, sessile to effused-reflexed, woody, white or pinkish poroid basidiocarps, possessing dimittic to trimitic hyphal system consisting of clamped generative hyphae, presence or absence of cystidial elements, and ellipsoid to subglobose thin-walled hyaline basidiospores, showing negative reaction to Melzer's reagent, it mainly causes a brown rot to a variety of hosts^[5,12,16,17]. Based on Hattori & Sotome, approximately 40 distinct species have been identified within *Fomitopsis*^[18]. Many species are found in North America, Europe, and East Asia^[9,19–27]. The phylogeny of *Fomitopsis* has long been debated, resulting in multiple taxonomic revisions and extensive investigations. In a comprehensive study conducted by Han et al.^[20], it was discovered that *Fomitopsis* s.l. does not form a monophyletic group. Instead,

numerous species within this group exhibit a close relationship with the brown-rotting species of *Antrodia* and *Daedalea*^[4,28]. Such observations prompted a reevaluation, leading to the recognition of distinct genera of brown-rotting fungi. The 'rosea clade', primarily comprising *Fomitopsis rosea* (Alb. & Schwein.) P. Karst. and *Fomitopsis cajanderi* (P. Karst.) Kotl. & Pouzar, were reclassified under a new genus named *Rhodofomes* Kotl. & Pouzar^[4]. Additionally, other significant genera, such as *Fragifomes* B.K. Cui, M.L. Han & Y.C. Dai, *Niveoporofomes* B.K. Cui, M.L. Han & Y.C. Dai, *Rhodofomitopsis* B.K. Cui, M.L. Han & Y.C. Dai, *Rubellofomes* B.K. Cui, M.L. Han & Y.C. Dai, and *Ungulidaedalea* B.K. Cui, M.L. Han & Y.C. Dai, were recognized within *Fomitopsis* s.l. by Han et al.^[5].

The Hindu Kush Mountain range in Pakistan is a biodiversity hotspot, which is poorly documented^[29]. Recently, a variety of mushrooms have been reported^[30,31], but their molecular data is still scarce. We conducted a detailed examination of wood-rotting specimens belonging to two families, collected from Hindu Kush Mountain in Pakistan, based on morphological observations and two genetic markers analysis (internal transcribed spacer — ITS and nuclear large subunit ribosomal DNA — nrLSU). Two species new to science and three new records in Pakistan are proposed in this study.

Materials and methods

Morphological characterization

The current research examined voucher specimens obtained from high-altitude temperate forests in the Swat district, Khyber Pakhtunkhwa (KP) Province, Pakistan. This district is located within the Hindu Kush Mountain range between lat. 34°34'–35°55' N and long. 72°08'–72°50' E. Woody vegetation, dense forest, and humid climatic conditions of the forests favor the growth of many wood-rotting fungi. During regular surveys, polypore specimens were collected from the area. The ephemeral macroscopic characteristics of basidiocarps were carefully documented in a field notebook. Terminologies introduced by Petersen were utilized to describe colors^[32]. All studied specimens were carefully dried at a temperature between 30 to 35 °C for 72 h until constant weight was obtained as suggested by Hu et al.^[33] and deposited at the herbarium of the University of Malakand, Pakistan (BGH).

The basidiocarps were subjected to microscopic examination using the methods and techniques outlined in previous studies^[14,34]. The standard notations described by Ji et al. were used for documentation^[34]. Freehand anatomical sections were prepared and analyzed under a microscope at magnifications up to 1,000×. The hyphal system, septal features, hymenial elements, and spore characteristics were studied in detail. Reagents such as 5% KOH, lactophenol cotton blue (CB), and Melzer's reagent (IKI) were employed to test for basidiospore staining. The resulting reactions were categorized as amyloid or Melzer's-positive (IKI+) if basidiospores showed staining, or inamyloid or Melzer's-negative (IKI–) for a negative reaction. The presence or absence of cyanophilic reaction was determined, and CB– denotes acyanophilous samples and CB+ for cyanophilous samples, following the classification by Banik et al.^[35]. The mean spore length (L) and width (W) were calculated by determining the arithmetic average of all measured spores. The variation in the length-to-width ratios (L/W) among the specimens examined was represented as Q. The spore

measured, denoted as 'n(a/b)', where 'a' represents the number of spores studied and 'b' the total number of specimens examined. Measurements of various structures were conducted using Image J software^[36].

DNA extraction

For gDNA extraction, a standardized CTAB method was followed with some modifications^[37–39]. Around 50 mg of a pore surface piece was homogenized in 400 µl of a 2% CTAB buffer containing 0.2% β-mercaptoethanol using a multi-beads shaker. The homogenate was then incubated at 65 °C for 1 h and added with 350 µl of chloroform: isoamyl alcohol (24:1) and then vortexed until a cloudy white mixture was obtained. Subsequently, the solution was centrifuged at 13,200 rpm at 4 °C for 20 min. The resulting supernatant, at the aqueous phase, was carefully transferred to a new autoclaved microtube. For the precipitation of DNA, 133 µl of ice-cold isopropanol was added to the supernatant, followed by centrifugation at 13,200 rpm at 4 °C for 20 min. The supernatant was discarded, and the resulting DNA pellet was washed twice by adding 500 µl of ice-cold ethanol. After each addition, the mixture was briefly vortexed and centrifuged for 3 min. The resulting pellet was air-dried and subsequently re-suspended in 100 µl of distilled water. The DNA extract was preserved at –20 °C until further use. The quantity and purity of the DNA extracts were assessed using the NanoDrop 1000 Spectrophotometer V3.7 (Thermo Fisher Scientific, Wilmington, DE, USA).

PCR and Sanger sequencing

The entire ITS and partial nrLSU regions were PCR-amplified on an Applied Biosystems Veriti thermal cycler using PuReTaq Ready-To-Go PCR Beads (GE Healthcare, Buckinghamshire, UK). The primer pairs used for ITS and nrLSU regions amplification were ITS1/ITS4 and LROR/LR5, respectively^[39–41]. The PCR reaction mixture (total vol. of 20 µl), consisted of 2 µl of genomic DNA (approx. 100 ng), 0.5 µl of each forward and reverse primer, 2.6 µl of Taq PCR buffer (10X), 11.4 µl of sterile deionized water (Fisher Scientific), 0.5 µl of Taq DNA polymerase from Takara BIO INC., 2.0 µl of MgCl₂, and 0.5 µl of dNTPs. The following thermocycling parameters were used for the amplification: initial denaturation at 95 °C for 5 min followed by 35 cycles of 95 °C for 30 s, 55 °C for 30 s, and 72 °C for 30 s and a final extension step performed at 72 °C for 8 min^[42]. Negative controls were included in the PCR reactions to ensure the absence of contamination. The PCR products were then run on an ethidium bromide-stained 1% agarose gel (Fisher Scientific, Waltham, MA, USA). A 1 Kb DNA ladder from Promega was used as a size reference to estimate the size of the amplified bands. After purification of the PCR products using the MEGA quick-spin™ PLUS Total Fragment DNA Purification Kit from Thermo Fisher Scientific, Sanger sequencing was performed at the sequencing facility of Macrogen Inc. in Seoul, South Korea (<https://dna.macrogen.com>). The purified PCR products were sequenced using the BigDye Terminator v3.1 cycle sequencing method.

Phylogenetic analyses

To confirm the identity of query nucleotide sequences, each sequence fragment was subjected to an individual Basic Local Alignment Search Tool (BLAST)^[43]. An initial dataset was obtained by retrieving and examining all publicly available ITS sequences in GenBank of NCBI under the query genera^[44]. To ensure the correct identification and retrieval of the right

reference sequences, protocols recommended by Nilsson et al.^[45] and Schoch et al.^[46] were followed. Specimen names associated with valid herbarium codes were included in the final data set.

Multiple alignments of the final data set were performed using an online version of MAFFT v. 7 software^[47]. The alignment was manually adjusted by removing gaps and ambiguous sites using BioEdit 7.2.5 software^[48], using methods from Shen et al.^[49]. The outgroup taxa *Perenniporia ochroleuca* (Berk.) Ryvarden and *Perenniporia medulla-panis* (Jacq.) Donk were used, following Soares et al.^[22]. Three phylogenetic analyses were performed on the combined ITS + nrLSU data set^[34,50]. The maximum parsimony (MP) analysis encompassed 1,000 iterative heuristic search replicates, employing random addition of taxa searches alongside tree-bisection-reconnection (TBR) branch exchanges. A consensus tree following the 50% majority rule was constructed, and the tree topology was assessed by computing parameters such as tree length, consistency index (CI), homoplasy index (HI), and retention index (RI)^[3].

The maximum likelihood (ML) analysis was performed using IQ-TREE version 1.6.12^[51]. To compute the best-fit substitution model via the Akaike information criterion (AIC), jModelTest was used^[52]. The final tree was inferred using 1,000 bootstrap values and setting all the base frequencies and substitution parameters as stated by Hoang et al.^[53]. The Bayesian Metropolis-coupled Markov Chain Monte Carlo (MCMCMC) inference was employed through MrBayes version 3.1^[54]. For each partition, substitution models were defined as *nst* = 6, rates = *invgamma* (ITS), and *nst* = 6, rates = *invgamma* (nrLSU). Model parameters, such as base frequencies, substitution rates, gamma shape, and *p.inv.*, were set for each partition accordingly. The analysis involved an operation of four chains throughout two million generations. Trees were sampled at an interval of 100 generations. The initial 5,000 trees (25% of the total) were excluded as burn-in, and the consensus tree was constructed from the remaining samples. The stop rule was set at *stopval* = 0.01^[55]. The generated tree was visualized using FigTree v1.4.2 (<http://tree.bio.ed.ac.uk/software/figtree/>) and subsequently subjected to editing. The ideal topologies derived from ML analysis were exhibited and verified using thresholds of ML-BS score (≥ 75), MP-BS score (≥ 50), and Bayesian posterior probabilities (BPPs) (≥ 0.95)^[34].

Results

The phylogenetic relationships of the species were analyzed using three methods: MP, ML, and Bayesian analysis. All inferred trees for each region were largely congruent, leading us to combine the matrices for further analysis. The results from the ML analysis are presented in Fig. 1, showing bootstrap proportion (MP), bootstrap (ML), and BPP values. The dataset consisted of 198 sequence variants, 99 ITS and 67 nrLSU sequences, including our subject sequences (Table 1). This added up to 37 species, with *Perenniporia ochroleuca* (Berk.) Ryvarden and *Perenniporia medulla-panis* (Jacq.) Donk serving as outgroup taxa. The concatenated data matrix, after alignment, consisted of 1,458 nucleotide characters, including gaps. Of these, 928 (86.3%) characters remained constant, 101 (4.91%) were variable or singleton sites considered parsimoniously uninformative, and 429 (8.8%) were parsimony informative characters, with a total of 552 distinct patterns. During the heuristic search of MP analysis, tree-bisection-reconnection

(TBR) branch swapping was employed, resulting in 100 equally parsimonious trees on one island. From these trees, a 50% majority rule consensus parsimonious tree was constructed, with the following description: tree length = 2,138, consistency index = 0.394, retention index = 0.818, rescaled consistency index = 0.322, and homoplasy index = 0.606. A two-partition dataset (ITS + nrLSU) was used for the ML analysis, and the initial log-likelihood was −11,213.440. The best evolutionary models for the ITS and nrLSU regions were GTR+I+G, with estimated gamma shape parameters of 0.6590 and 0.4810, and *p*-invariance values of 0.2310 and 0.4950, respectively. The analysis converged after 20,000,000 generations, with a standard deviation of split frequencies of 0.009983. The results from both the Bayesian and likelihood analyses exhibited similar topologies and clade distributions.

Based on molecular and morphological analyses, two new species were confirmed: one in *Climacocystis* and the other in *Rhodofomes*. The sample sequence MUSI21-41 forms a distinct and independent lineage within *Climacocystis*, receiving strong support (100% MP, 100% ML, and 1.00 BPP). In addition, it differs significantly in microscopic characteristics from the two well-supported species within the genus, namely *C. montana* B.K. Cui & J. Song and *C. borealis* (Fr.) Kotl. & Pouzar. Similarly, the sample sequence MU1E exhibited robust clustering with significant support (71% MP, 97% ML, and 1.00 BPP) within the *Rhodofomes* clade. However, it is noteworthy that this sequence forms an independent lineage, distinctly separate from other known *Rhodofomes* species. Despite some morphological similarities with the known species within the genus, a few characteristics are unique to this new description.

Additionally, through phylogenetic analysis, three polypores new to Pakistan were identified. MUBS40 corresponds to *Daedalea dickinsii* Yasuda. This assignment received substantial phylogenetic support (88% MP, 100% ML, and 1.00 BPP). Specimens examined under MUJMK14 are classified as *Neoantrodia serialis* (Fr.) Audet, with strong support values (98% MP, 100% ML, and 1.00 BPP). Finally, the sample MUBS85 groups together with *Rhodofomes roseus* (Alb. & Schwein.) Kotl. & Pouzar, showing significant support values (87% MP, 98% ML, and 1.00 BPP) (Fig. 1). The morphological characteristics of these three species from Pakistan corresponded to each of the descriptions of type specimens.

Taxonomy

Climacocystis temperata S. Hussain, M. Nisar & Y.W. Lim sp. nov.

Mycobank no.: MB852033

Holotype: *Climacocystis temperata*, voucher no. MUSI21-41, PAKISTAN, KP PROVINCE, Sialkot, Swat District, (lat. 34°59'09" N and long. 72°10'55" E, 2,748 m a.s.l.) in mixed coniferous forest on dead tree inside the hollow stumps (6 feet) of *Abies pindrow* (Royle ex D. Don) Royle, July 29, 2021, MUSI21-41(BGH F000501), Mycology section of Botanical Garden Herbarium, University of Malakand (BGH). nrRNA gene sequences holotype: ITS (OR364522), nrLSU (OR364606).

Diagnosis: Distinguished from other *Climocystis* spp. by having larger (up to 19 cm wide) and leathery basidiocarp, with distinctly zonate pileal surface, pores 1–3 (usually 2)/mm, with entire to serrate margin, possessing varied shaped hymenial cystidia, elongated clavate basidia up to 47 μ m long, notably larger ellipsoid basidiospores (6.7–10.7 \times 3.9–6.1 μ m), showing *Q* = 1.40–1.51, and associated with *A. pindrow*.

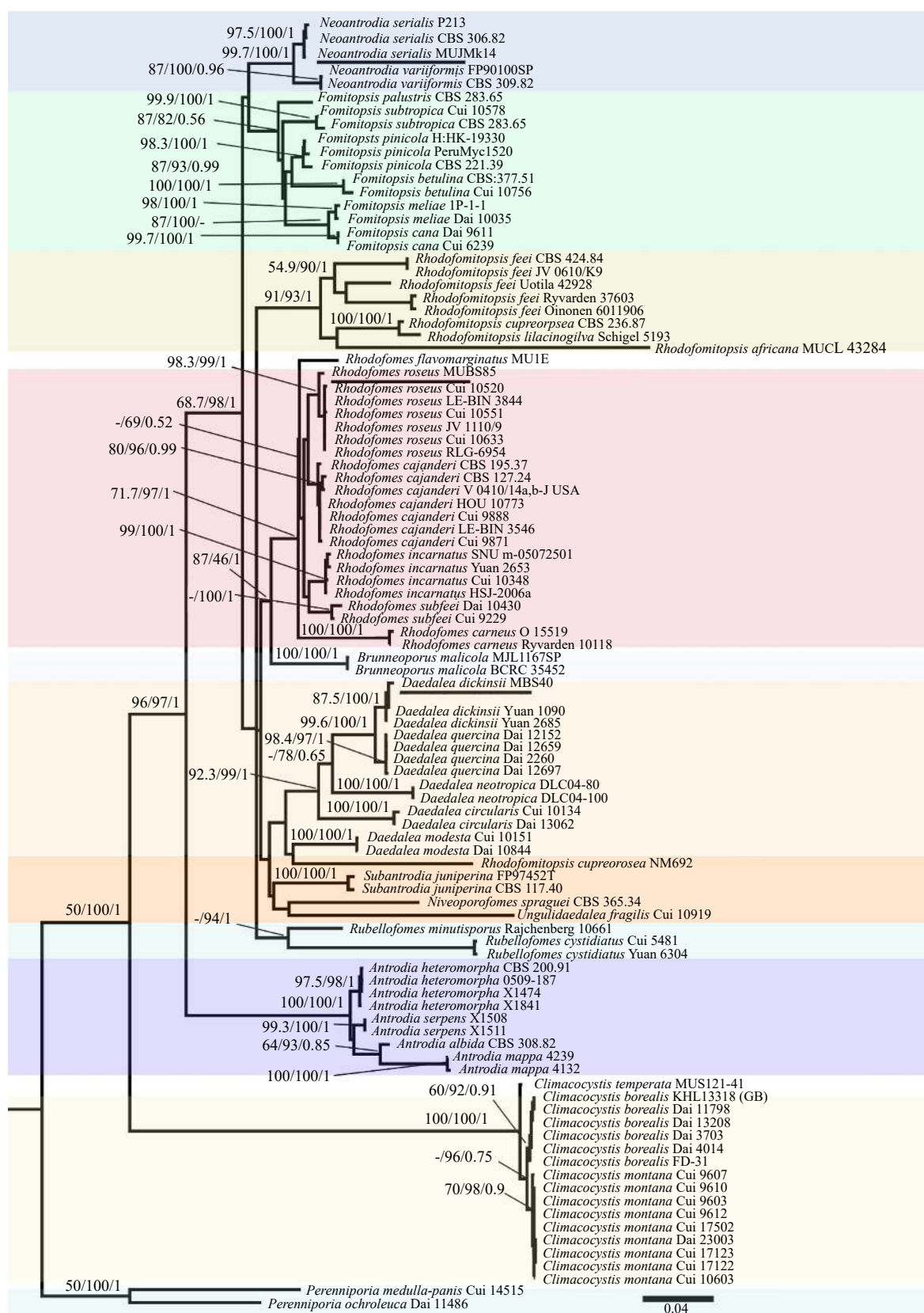


Fig. 1 ML consensus phylogenetic tree of species from brown-rotting genera including *Antrodia*, *Daedalea*, *Fomitopsis*, *Neoantrodia*, *Rhodofomes*, *Rhodofomitopsis*, and white-rotting *Climacocystis* species based on ITS and nrLSU sequences. Node support values are shown in the order of MP bootstrap/ML bootstrap/Bayesian posterior probabilities. Collection/voucher numbers are appended as tip labels and our specimens shown as underlined. Two new species *R. flavomarginatus* and *C. temperata* are indicated in bold and three previously unrecorded species in Pakistan are underlined.

Table 1. Names, collection numbers, and corresponding GenBank accessions of the taxa used in the phylogenetic analyses of this study.

| Taxa | Collection no./voucher | ITS | nrLSU | Origin |
|-----------------------------------|------------------------|----------|----------|----------------|
| <i>Antrodia albida</i> | CBS 308.82 | DQ491414 | NA | Korea |
| <i>A. serpens</i> | X1508 | KC543167 | NA | France |
| <i>A. serpens</i> | X1511 | KC543169 | NA | France |
| <i>A. heteromorpha</i> | CBS 200.91 | DQ491415 | NA | Korea |
| <i>A. heteromorpha</i> | 0509-187 | KC543121 | KC543121 | USA |
| <i>A. heteromorpha</i> | X1474 | KC543150 | KC543150 | Norway |
| <i>A. heteromorpha</i> | X1841 | KC543177 | KC543177 | Finland |
| <i>A. mappa</i> | Am4132 | KC543130 | KC543130 | Canada |
| <i>A. mappa</i> | Am4239 | KC543113 | KC543113 | Finland |
| <i>Brunneoporus malicola</i> | BCRC 35452 | DQ013299 | AY333837 | Taiwan |
| <i>B. malicola</i> | MJL11675P | AY966449 | NA | Taiwan |
| <i>Climacocystis borealis</i> | Dai 3703 | KJ566626 | KJ566636 | China |
| <i>C. borealis</i> | Dai 11798 | KJ566632 | KJ566641 | China |
| <i>C. borealis</i> | Dai 13208 | KJ566635 | KJ566642 | China |
| <i>C. borealis</i> | Dai 4014 | KJ566627 | KJ566637 | China |
| <i>C. borealis</i> | FD-31 | KP135308 | KP135210 | USA |
| <i>C. borealis</i> | KHL13318 (GB) | JQ031126 | NA | Sweden |
| <i>C. montana</i> | Cui 10603 | KJ566634 | NA | China |
| <i>C. montana</i> | Cui 17122 | ON682359 | ON680811 | China |
| <i>C. montana</i> | Cui 17502 | MW377276 | MW377356 | China |
| <i>C. montana</i> | Cui 9610 | KJ566630 | NA | China |
| <i>C. montana</i> | Cui 17123 | ON682360 | ON680812 | China |
| <i>C. montana</i> | Cui 9607 | KJ566629 | KJ566639 | China |
| <i>C. montana</i> | Cui 9612 | KJ566631 | KJ566640 | China |
| <i>C. montana</i> | Dai 23003 | ON682358 | OL423570 | China |
| <i>C. montana</i> | Cui 9603 | KJ566628 | KJ566638 | China |
| <i>C. temperata</i> | MUSI21-41 | OR364522 | OR364606 | Pakistan |
| <i>Daedalea circularis</i> | Cui10134 | JQ314352 | KP171221 | China |
| <i>D. circularis</i> | Dai 13062 | KP171200 | KP171222 | China |
| <i>D. dickinsii</i> | Yuan 1090 | KR605790 | KR605729 | China |
| <i>D. dickinsii</i> | Yuan 2685 | KP171201 | KP171223 | China |
| <i>D. dickinsii</i> | Yuan 2707 | KP171202 | KP171224 | China |
| <i>D. dickinsii</i> | MUBS40 | OM533594 | NA | Pakistan |
| <i>D. modesta</i> | Cui 10151 | KP171205 | KP171227 | China |
| <i>D. modesta</i> | Dai 10844 | KP171206 | KP171228 | China |
| <i>D. neotropica</i> | DLC04-100 | FJ403218 | NA | Belize |
| <i>D. neotropica</i> | DLC04-80 | FJ403217 | NA | USA |
| <i>D. quercina</i> | Dai 12659 | KP171208 | KP171230 | Finland |
| <i>D. quercina</i> | Dai 12697 | KP171209 | KP171231 | Czech Republic |
| <i>D. quercina</i> | Dai 2260 | KR605792 | KR605885 | China |
| <i>D. quercina</i> | Dai 12152 | KP171207 | KP171229 | China |
| <i>Fomitopsis betulina</i> | CBS:377.51 | MH856908 | MH868430 | China |
| <i>F. betulina</i> | Cui 10756 | KR605797 | KR605736 | China |
| <i>F. cana</i> | Cui6239 | JX435777 | JX435775 | China |
| <i>F. cana</i> | Dai9611 | JX435776 | JX435774 | China |
| <i>F. meliae</i> | 1P_1_1 | FJ372673 | FJ372695 | Thailand |
| <i>F. meliae</i> | Dai 10035 | KR605774 | NA | China |
| <i>F. palustris</i> | CBS 283.65 | DQ491404 | MH870206 | Korea |
| <i>F. pinicola</i> | CBS 221.39 | DQ491405 | NA | Korea |
| <i>F. pinicola</i> | H:HK-19330 | KF169655 | NA | Russia |
| <i>F. pinicola</i> | PeruMyc1520 | MG820763 | NA | Italy |
| <i>F. subtropica</i> | Cui 10578 | KR605787 | KR605726 | China |
| <i>F. subtropica</i> | Cui10140 | JQ067651 | NA | China |
| <i>Neonantrodia serialis</i> | CBS 306.82 | DQ491417 | NA | Korea |
| <i>N. serialis</i> | MUJMK14 | OR364518 | NA | Pakistan |
| <i>N. serialis</i> | P213 | AJ344139 | NA | Germany |
| <i>N. variiformis</i> | CBS 309.82 | DQ491418 | NA | Korea |
| <i>N. variiformis</i> | FP90100SP | AY966453 | NA | China |
| <i>Niveoporofomes spraguei</i> | CBS 365.34 | DQ491406 | NA | Korea |
| <i>Perenniporia medulla-panis</i> | Cui14515 | MW989399 | NA | China |
| <i>P. ochroleuca</i> | Dai11486 | HQ654105 | JF706349 | China |
| <i>Rhodofomes cajanderi</i> | CBS 127.24 | DQ491407 | MH866275 | Korea |
| <i>R. cajanderi</i> | CBS 195.37 | DQ491399 | NA | Korea |

(to be continued)

Table 1. (continued)

| Taxa | Collection no./voucher | ITS | nrLSU | Origin |
|---------------------------------|------------------------|----------|------------|----------------|
| <i>R. cajanderi</i> | Cui 9871 | KC507158 | KC507168.1 | China |
| <i>R. cajanderi</i> | Cui 9888 | KC507156 | KC507166 | China |
| <i>R. cajanderi</i> | HOU 10773 | DQ491413 | NA | Korea |
| <i>R. cajanderi</i> | LE-BIN 3546 | MG735350 | NA | Russia |
| <i>R. cajanderi</i> | V 0410/14a,b-J USA | KR605768 | KR605707 | USA |
| <i>R. carneus</i> | Leif Ryvarden 10118 | KF999921 | KF999925 | China |
| <i>R. carneus</i> | O 15519 | KC507155 | KC507165 | China |
| <i>R. cystidiatus</i> | Yuan 6304 | KR605769 | KR605708 | China |
| <i>R. flavomarginatus</i> | MU1E | OR364739 | OR364741 | Pakistan |
| <i>R. incarnatus</i> | Cui 10348 | KC844848 | KC844853 | China |
| <i>R. incarnatus</i> | HSJ-2006a | DQ491411 | NA | Korea |
| <i>R. incarnatus</i> | SNU m-05072501 | DQ491409 | NA | Korea |
| <i>R. incarnatus</i> | Yuan 2653 | KC844849 | KC844854 | China |
| <i>R. roseus</i> | Cui 10633 | KR605782 | KR605721 | China |
| <i>R. roseus</i> | Cui 10520 | KC507162 | AY333809 | China |
| <i>R. roseus</i> | Cui 10551 | KC507163 | KC507173 | China |
| <i>R. roseus</i> | JV 1110/9 | KR605783 | KR605722 | Czech Republic |
| <i>R. roseus</i> | LE-BIN 3844 | MG734829 | NA | Russia |
| <i>R. roseus</i> | MUBS85 | OR364705 | OR364719 | Pakistan |
| <i>R. roseus</i> | RLG-6954 | KC585353 | KC585181 | USA |
| <i>R. subfeei</i> | Cui 9229 | KR605789 | KR605728 | China |
| <i>R. subfeei</i> | Dai 10430 | KR605788 | KR605727 | China |
| <i>Rhodofomitopsis africana</i> | MUCL 43284 | DQ491422 | NA | Cameroon |
| <i>R. cupreorosea</i> | CBS 236.87 | DQ491400 | AY515325 | Costa Rica |
| <i>R. cupreorosea</i> | NM692 | MF589757 | MF590128 | Brazil |
| <i>R. feei</i> | CBS 424.84 | DQ491402 | NA | Korea |
| <i>R. feei</i> | JV 0610/K9 | KF999922 | KF999926 | Kout Mexico |
| <i>R. feei</i> | Oinonen 6011906 | KC844851 | KC844856 | Brazil |
| <i>R. feei</i> | Ryvarden 37603 | KC844850 | KC844855 | Venezuela |
| <i>R. feei</i> | Uotila 42928 | KF999924 | KF999928 | Australia |
| <i>R. lilacinogilva</i> | Schigel 5193 | KR605773 | KR605712 | Australia |
| <i>Rubellofomes cystidiatus</i> | Cui 5481 | KF937288 | KF937291 | China |
| <i>R. minutisporus</i> | Rajchenberg 10661 | KR605777 | KR605716 | Argentina |
| <i>Subantrodia juniperina</i> | FP97452T | AY966454 | NA | Taiwan |
| <i>S. juniperina</i> | CBS 117.40 | DQ491416 | MH867551 | USA |
| <i>Ungulidaedalea fragilis</i> | Cui 10919 | KF937286 | NG_060408 | China |

* NA = Not available.

Etymology: 'temperata' is a Latin word characterizing the distribution of *C. borealis* and *C. montana* in the temperate forests, used in analogy with the other species of the genus.

Description: Basidiocarps are large sized, annual, imbricate, connate at the attachment, dimidiate to applanate, laterally stipitate, substipitate or almost sessile, thick fleshy and leathery textured, watery, becoming lightweight and hard woody when dry, having a distinct pungent odor and acidic flavor. Pilei growing up to 5–12 cm long, 10–19 cm wide, and 1.5–3.5 cm thick at the attachment point, hairy, showing distinct margins up to 2.5 mm of white colored; upper surface plano-concave, whitish or pale to cream-colored, distinctly zonate in mature basidiocarp, furrowed or striated along the radii, tomentose or somewhat velutinate, becoming dull yellowish brown when dry. Margin whitish, sterile, smoothly blunt, and entire to serrate in mature basidiocarp, distinct on both surfaces up to 2.5 mm wide. Stipe almost absent or with short robust stipe. Pore surface pale yellow when fresh, bruises brown to clay buff when dry, rounded to radially elongated (reaching up to 1.8 mm long), or elliptic and irregularly distributed. Pore lining first rounded then more or less elliptical angular, number of pores 1–3 (2) mm⁻¹; dissepiment 0.2–1.12 (0.49) mm in thickness, and

usually lacerate. The tube layer is detachable, yellow to pale-colored, and up to 3 mm at the widest point. Context whitish showing prominent radial ridges when the tube layer is peeled up, becoming spongy when dry, context up to 1.5 cm thick at the widest point, distinctly colored from the tube layer (Fig. 2).

Hyphal system monomitic; generative hyphae in the tube and context layer are IKI–, CB– unaffected by KOH. The contextual hyphae are light yellow or rarely hyaline, usually branched, occasionally septate, frequently clamped (compound clamps) showing interwoven, subparallel arrangement, 5.2–8.1 (6.5) µm in diam. Hymenial cystidia, 22.8–58.5(39.8) × 3.8–9.4(6.1) µm, variable in shape, often capitated, ventricose, rarely hyphoid, basally septate, smooth, thinwalled, usually yellowish colored, lacking encrustation. Basidia long, clavate, granular yellowish content, with four short sterigmata and basal clamp, 21.5–47.6(33.8) × 5.4–8.2(6.6) µm (n = 35/3). Basidiospores are ellipsoid shaped, thin, smooth, uniguttulate with hyaline lining, non-dextrinoid, acyanophilous, varied size, 6.7–10.7 × 3.9–6.1 µm, L = 7.72 ± 0.35 µm, W = 5.34 ± 0.51 µm, Q = 1.40–1.51 (n = 90/3) (Fig. 3).

Additional specimens cited: Vouchers including MUSI23-40 (lat. 34°59'27" N and long. 72°10'52" E, 2,935 m a.s.l., on stump



Fig. 2 Basidiocarps of *Climacocystis temperata* (a), (b), (c) from its natural habitat; (d) close-up view of the pileal surface (fresh); (e) pore surface; (f) cross sectional view of fresh specimen showing yellow tube layer and white context. Scale bars: (a), (d) = 1 cm; (b), (c) = 2 cm; (e) = 4 mm; (f) = 5 mm.

of *A. pindrow*), MUSI23-27 (lat. 34°59'36" N and long. 72°10'54" E, 2,895 m a.s.l., on stump of *A. pindrow*) were collected from the type locality and examined for the morpho-anatomical characterization.

***Rhodofomes flavomarginatus* S. Hussain, M. Nisar & Y.W. Lim sp. nov.**

Mycobank no.: MB852034

Holotype: *Rhodofomes flavomarginatus*, voucher No. MU1E, PAKISTAN, KP PROVINCE, Malam Jabba, district Swat, (lat. 34°47'37" N and long. 72°34'38" E, 2,680 m a.s.l.) in the mixed coniferous forest on dead tree stumps (7 feet) of *Abies pindrow* (Royle ex D.Don) Royle, 1st September, 2016, MU1E (BGH F000502), Mycology section of Botanical Garden Herbarium, University of Malakand (BGH), nrRNA gene sequences holotype: ITS (OR364739), nrLSU (OR364741). Rarely distributed in the type locality.

Diagnosis: This species differs from other *Rhodofomes* species by having large, thick, woody perennial, ungulate basidiocarps with clearly broad, obtuse, yellow-colored margins, possessing dimitic hyphal construct, short, broadly clavate basidia, 6.3–16.7(11.7) × 3.5–5.7(4.8) µm, rare occurrence of cystidioles and slightly small sized basidiospore (5.5–6.0 × 2.9–3.2 µm).

Etymology: 'flavomarginatus' is a Latin word combining 'flavus' and 'marginatus', signifying the yellow bordered basidiocarps of the species.

Description: Basidiocarps pileate, perennial, sessile to effused reflexed, solitary, ungulate, dimidiate or semicircular on the underside, hard, woody textured, becoming lightweight when dry, indistinct odor and taste. Pileus 14 cm long, 10 cm wide, 20 cm thick at the base; upper surface dark grayish brown, becoming dull brown when dry, glabrous, azonate

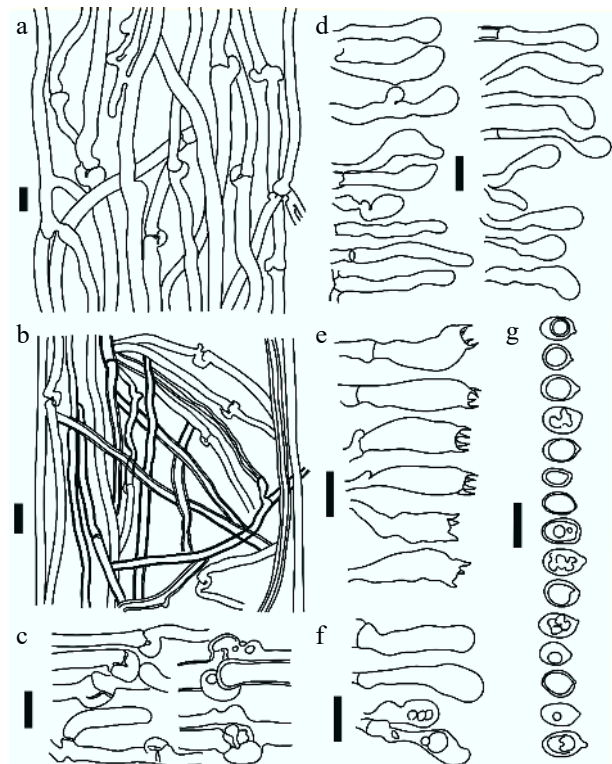


Fig. 3 Drawing from the microscopic examination of holotype specimen of *Climacocystis temperata*. (a) Contextual generative hyphae showing branches and clamps; (b) tramal monomitic hyphal construct showing generative hyphae; (c) simple and compound clamp connections; (d) hymenial cystidia of different shapes; (e) basidia; (f) basidioles; (g) basidiospores showing different aspect view. All scale bars are 10 µm.

surface with 1–2 deep grooves or fissures behind the margin. Margin rounded, smooth, sterile, blunt, undulating, forming over-grown rim beyond the pileal and hymenophore surface, yellow color, fading to light ochraceous when dry, 3–4 cm wide. Stipe absent, broadly attached to the wood but easily separable from the substrate. Pore surface pinkish white, tuberculate, producing amber to red colored exudates, pores minutes (0.05–0.19 mm in diam.), mostly rounded, irregular in distribution, pore-lining entire, number of pores 5–6(5) mm⁻¹; dissepiment uniform in thickness 0.16–0.31 mm. Tube layer tightly affixed to the context, striated or multilayered, dark brown colored, each layer 2–3 mm thick. Context brownish, fibrous, or cottony, up to 5 cm in thickness (Fig. 4).

Hyphal structure dimitic both in context and hymenophore of the basidiocarp; skeletal hyphae predominate in the context, 3.3–7.4(5.4) µm in diam (n = 40/1), rarely branched, non-septate, yellowish to dark brown in KOH, solid to semisolid, interwoven; generative hyphae found both in trama and context, usually dominating in the trama, branched, clamped, septate, light yellow to hyaline, thin-walled, ranging 2.6–3.9(3.2) µm in diam (n = 43/1), interwoven arrangement. Basidia small sized, broadly clavate, with short 4 sterigmata and a basal clamp, 6.3–16.7(11.7) × 3.5–5.7(4.8) µm (n = 28/1). Cystidioles club shaped, 23.2–30.6(27.3) × 3.4–4.2(3.9) µm, rarely observed. Basidiospores cylindric to ellipsoid, straight, hyaline, thin, smooth, non-dextrinoid, acyanophilous, 5.1–6.0 × 2.6–3.1 µm, L = 5.54, W = 2.97 µm, Q = 1.86 (n = 32/1) (Fig. 5).

***Daedalea dickinsii* Yasuda, Bot. Mag., Tokyo 36: (128) (1922)**

Mycobank no.: MB481905

Vouchers: PAKISTAN, KP PROVINCE: (i) *Daedalea dickinsii* voucher No. MBS40, Sailand, district Swat, (34°59'48" N and 72°11'07" E, 2,888 m a.s.l.), mixed coniferous forest on living

trees and dead tree stumps of *Quercus semecarpifolia* Sm., August, 2020, MBS40 (BGH F000503), Mycology section of Botanical Garden Herbarium, University of Malakand (BGH).

Description: Basidiocarps are small, perennial, effused-reflexed, imbricate, dimidiate, unguulate, broadly sessile thick corky textured or coriaceous, becoming woody when dry, having a distinct pungent odor and acidic flavor. Pilei 3–4 cm long, 5–6 cm wide, 1–2 cm thick at the broader base; upper surface velutinate, brown or buff brown, becoming greyish brown or dull brown when dry, distinctly zonate, sulcate, concentric zonation at growing margin distinctly yellow. Margin whitish or pale, sterile, smoothly rounded, and blunt or obtuse up to 1 cm wide, fading to light brown when dry. The stipe are almost absent but broadly attached to the exposed wood. Hymenophoral surface ochraceous or light brown or cream when fresh, becoming brown when dry; pores mostly rounded or angular and irregularly distributed, labyrinthine or daedaleoid, elongated and deep towards the base and shallow to the growing margin, number of pores 1–2(2) mm⁻¹; dissepiment 0.3–0.9 mm in thickness, and usually entire. The tube layer is tightly affixed to the context, whitish brown colored in the young layer and light brown in the older layers, about 1–1.5 cm thick, almost concolorous with pore surface. Context multilayered or zonate showing thin cuticle layer; tubes light brown, coriaceous, spongy on drying, 0.3–0.8 cm at the widest point near the attachment. Context to tube layer ratio is 1–2.5:1. Indistinct taste and odor (Fig. 6).

Rot type: brown-rotting

Hyphal system dimitic; skeletal hyphae dominant in the context layer, IKI–, CB–, range 3.1–6.3(5.0) µm (n = 35/1) characterized by hyaline, rarely branched, non-septate, interwoven; generative hyphae 2.6–4.0(3.2) rarely observed in the context. Basidia, clavate, with short sterigmata, 12.9–28.8(20.8) ×



Fig. 4 Basidiocarps of *Rhodofomes flavomarginatus* (a), (c) from its natural habitat showing pileal surface; (b), (d) close-up view of pores surface (fresh) showing exudates. Scale bars: (a), (b), (d) = 1 cm; (c) = 5 cm.

Characterization of wood-decaying polypore

3.2–5.4(4.4) μm ($n = 40/1$). Cystidiales are fusoid or tubular, thin-walled, hyaline, septated at the base 13.2–24.9(18.2), rarely observed. Basidiospores narrowly cylindrical, thin-walled,

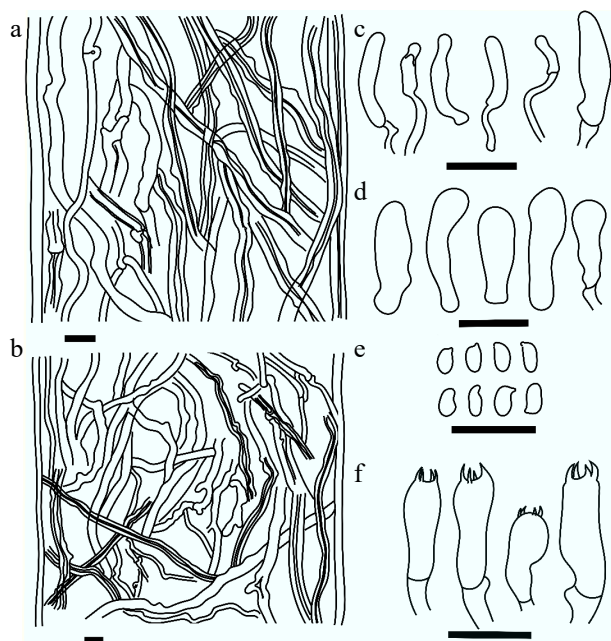


Fig. 5 Microscopic structures drawn from holotype specimen of *Rhodofomes flavomarginatus*. (a) Context showing generative and skeletal hyphae; (b) dimitic hyphal construct from trama; (c) cystidiales; (d) basidioles; (e) basidiospores; (f) basidia. Scale bars are 10 μm .

non-dextrinoid, acyanophilous, 6.6–11.3 \times 2.7–3.9 μm , $L = 9.71 \mu\text{m}$, $W = 3.48 \mu\text{m}$, $Q = 2.79$ ($n = 32/1$) (Fig. 6).

***Neoantrodia serialis* (Fr.) Audet, Mushrooms nomenclatural novelties 6: [2] (2017)**

Mycobank no.: MB552864

Vouchers: PAKISTAN, KP PROVINCE: (i) *Neoantrodia serialis* voucher No. MUJMK14, Jabba Mankyal, district Swat, (35°19'26" N and 72°39'26" E, 2,650 m a.s.l.), mixed coniferous forest on downed and dead tree logs of *Abies pindrow* (Royle ex D. Don) Royle, July, 2019; (ii) *Neoantrodia serialis* voucher No. MUJMK14b, Jabba Mankyal, district Swat, (35°20'53" N and 72°40'50" E, 2,563 m a.s.l.), mixed coniferous forest on sloping tree logs of *Picea smithiana* (Wall.) Boiss., July, 2020, MUJMK14 (BGH F000504), Mycology section of Botanical Garden Herbarium, University of Malakand (BGH).

Description: Basidiocarps large sized, annual to perennial, usually completely resupinate, evenly flat, covering up to 80 \times 40 cm of the substrate surface, very rarely reflexed, closely affixed or adnate to the downed logs or partly detaching at the senescent portion, about 3–4 mm thick, margin compact or slightly upwardly curved, wavy margin up to 0.5 mm thick and indistinct at other parts; pore surface regular, white or cream, becoming pale brown when dry, pores regular, rounded, 3–5(3) mm^{-1} , soft leathery textured becoming woody and lightweight when dry; tubes layer concolorous with pore surface, 2–3.5 mm thick, non-stratified; dissepiment thin and entire; odor unrecorded, taste bitter (Fig. 7). Context white, 0.1–0.3 mm.

Hyphal system dimitic: skeletal hyphae were prominent, solid or semisolid (with capillary to fairly wide lumen), rarely branched and accidentally septated, 2.6–5.1(3.5) μm in diam.

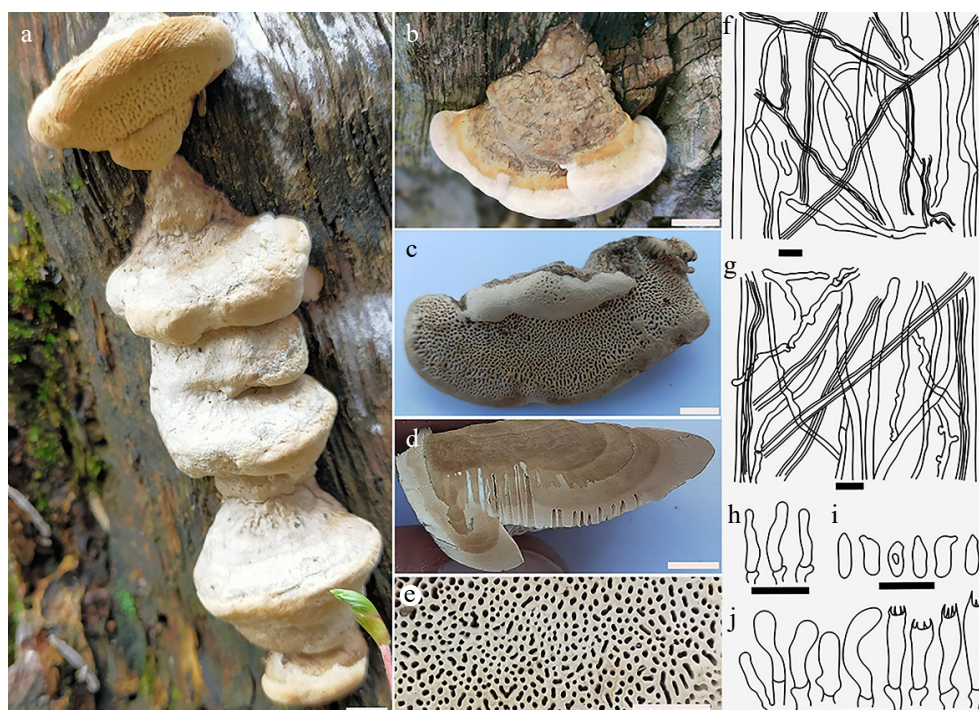


Fig. 6 Basidiocarps of *Daedalea dickinsii* (a) from its natural substrate; (b) pileal surface, also showing margin; (c) pore surface (dried); (d) cross section showing context and tube layers; (e) close-up view of pores; (f) microscopy of context showing skeletal and generative hyphae; (g) skeletal and generative hyphae from trama; (h) cystidiales; (i) basidiospores; (j) basidioles and basidia. Scale bars: (a)–(d) = 1 cm; (e) = 5 mm; (f)–(j) = 10 μm .

($n = 38/2$), thick-walled, interwoven; generative hyphae abundant, yellowish, thin-walled, branched, rarely septate and clamped, occasionally inflated and tortuous, $2.4\text{--}4.9(3.9) \mu\text{m}$ in

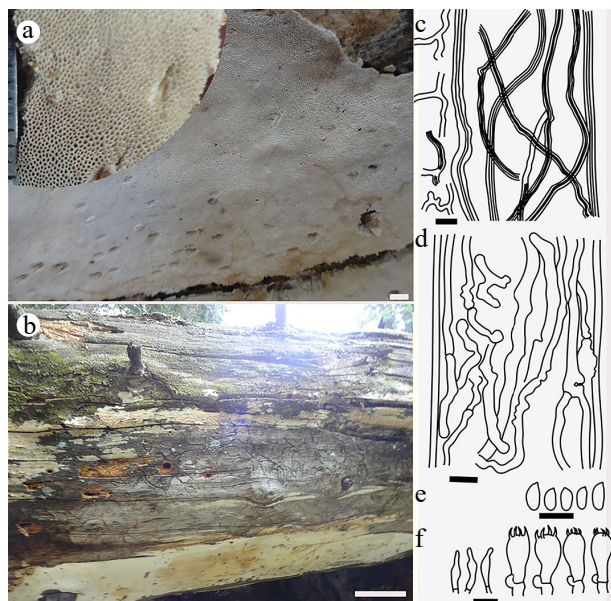


Fig. 7 Basidiocarps from *Neoantrodia serialis*. (a) Pore surface showing close-up view of pores; (b) resupinate basidiocarp adnate to the substrate; (c) skeletal and generative hyphae of context showing branches; (d) generative hyphae from the trama showing separation and branching; (e) basidiospores; (f) basidia and hyphoid cystidia. Scale bars: (a) = 5 mm; (b) = 10 cm; (c)–(f) = $10 \mu\text{m}$.

diam. ($n = 42/2$). Cystidia frequently occurring, deeply located skeletocystidia possessing clavate apices and thick-walled, $10.6\text{--}18.7 \times 3\text{--}5.5 \mu\text{m}$ with hyphoid cystidioles. Basidia broadly clavate, agglutinated, with short 4-sterigmate and a basal clamp, $10.2\text{--}15.8(13.6) \times 4.5\text{--}7.2(5.4) \mu\text{m}$. Basidiospores are narrowly cylindrical to oblong, thin-walled, non-dextrinoid, acyanophilous, tapering towards the distal end, $5.6\text{--}8.7 \times 2.2\text{--}3.2 \mu\text{m}$, $L = 6.52 \pm 0.34 \mu\text{m}$, $W = 2.81 \pm 0.55 \mu\text{m}$, $Q = 2.16\text{--}2.45$ ($n = 65/2$). Large sized diffused crystals were also found in the tramal tissue (Fig. 7).

Rot type: brown-rotting

***Rhodofomes roseus* (Alb. & Schwein.) Kotl. & Pouzar, Česká Mykol. 44 (4): 235 (1990)**

Mycobank no.: MB127496

Vouchers: PAKISTAN, KP PROVINCE: *Rhodofomes roseus* voucher No. MUBS85, Sailand, Swat District, ($34^{\circ}59'22''$ N and $72^{\circ}10'56''$ E, 2,833 m a.s.l.), mixed coniferous forest on living trees and dead tree stumps of *Abies pindrow* (Royle ex D. Don) Royle, August, 2020, MUBS85 (BGH F000505), Mycology section of Botanical Garden Herbarium, University of Malakand (BGH).

Description: Basidiocarps, annual, perennial, effused reflexed, solitary, pileate dimidiate to applanate, semicircular, sessile to broadly attached, hard, woody, tough textured, becoming lightweight when dry, having indistinct odor and taste. Pilei 2–4 cm long, 5–8 cm wide, and 1 cm thick at the base, upper surface dark brownish, light pinkish brown towards the margin, showing blackish stains, glabrous, azonate surface no groove or fissure observed, Margin acute to rounded, smooth, sterile, blunt, undulating, indistinct on both surfaces, light pink brownish or clay pink. Stipe absent, broadly attached to the woods. The pore surface is pinkish white or rosaceous, producing cream colored exudates, pores minutes mostly

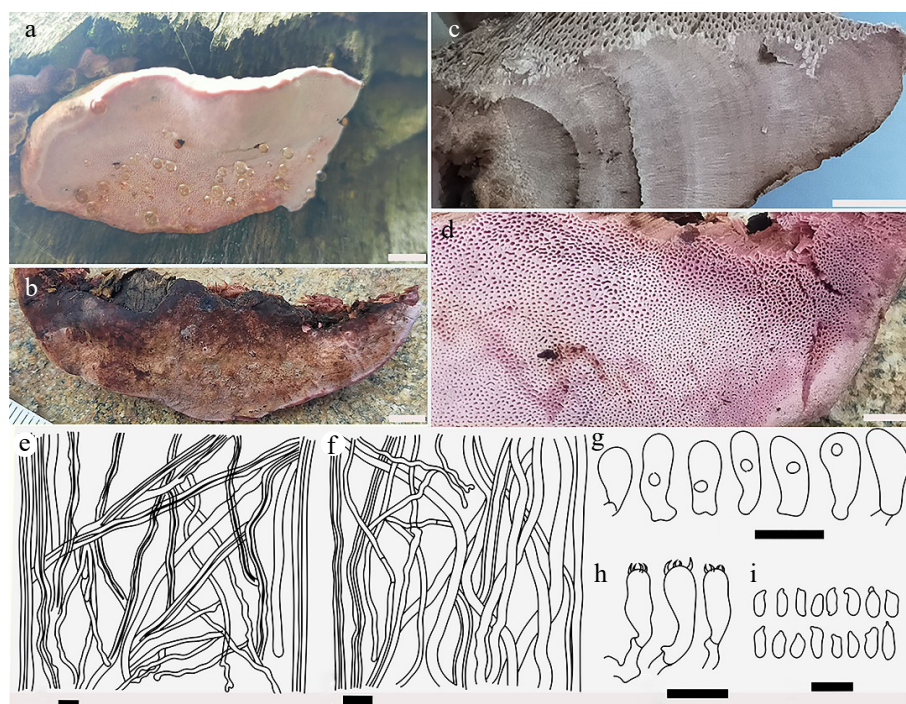


Fig. 8 Basidiocarps of *Rhodofomes roseus* (a) from its natural habitat showing pore surfaces and margin; (b) view of pileal surface; (c) cross section view of fresh specimen depicting zonation; (d) close-up view of pores; (e) dimittic construct of context showing dominant skeletal hyphae and generative hyphae; (f) skeletal and generative hyphae from trama; (g) basidioles; (h) basidia; (i) basidiospores. Scale bars: (a), (b) = 1 cm; (c) = 5 mm; (d) = 2 mm; (e)–(i) = $10 \mu\text{m}$.

Characterization of wood-decaying polypore

rounded to elliptical and irregular in size (0.04–0.36 mm in diam.) and distribution. Pore lining entire, number of pores 5–6(4) mm⁻¹; dissepiment non-uniform in thickness 0.1–0.3 mm. Tube layer tightly affixed to the context, striated or multi-layered dark brown colored, 4–4.5 mm thick. Context brownish, fibrous, pinkish white to light brown color, up to 7–9 mm thick at the attachment with distinct cuticle of pileal surface. Section exhibits distinctive zonation and layers representing seasonal growth variation (Fig. 8).

Hyphal system dimitic both in the context and hymenophore; skeletal hyphae indeterminate, rarely branched, non-septate, hyaline, thick-walled, interwoven, 2.9–6.1 (4.6) µm in diam; generative hyphae predominant in the trama, branched, rarely clamped, septate, light yellow, thin-walled, ranging 2.7–5.4(3.8) µm in diam, interwoven arrangement. Basidia clavate to broadly cylindrical, with short sterigmata and a basal clamp, 7.2–16.2(11.9) × 3.7–5.9(4.8) µm. Basidioles frequently small sized, pyriform to globose shaped 9.2–12.7(11) × 3.3–5.6(4.8) µm. Cystidial elements were not found. Basidiospores oblong to cylindric, hyaline, thin-walled, non-ditrid, acyanophilous, varied in size, 5.5–7.7 × 2.3–3.6 µm, L = 5.84 µm, W = 2.72 µm, Q = 2.15 (n = 32/1) (Fig. 8).

Rot type: brown-rotting

Discussion

The analyses of both morphoanatomical characteristics and phylogenetic data of the collected specimens revealed noteworthy findings, contributing three new records to Pakistan and two novel species. The species examined in this study are distributed across distinct clades within two families, *Fomitopsidaceae* and *Climacocystaceae*, located within the Polyporales^[4,28]. The inferred phylogeny of the species highlights their interrelationship in the broader context (Fig. 1). Phylogenetically, our findings additionally corroborate the clustering of brown-rotting genera, as indicated in previous studies^[20,21,28,56,57]. Nevertheless, certain branches in the heterogeneous brown-rotting cluster exhibited limited resolution^[4,8,58]. These species may be distinguished morphologically (Table 2).

The combined data from both nrRNA genes (ITS + nrLSU) showed two large groups of clades, each consisting of a single new species reported in this study. The group of *Anurodia* s.l.-*Daedalea* s.l.-*Fomitopsis* s.l. all comprised brown-rotting genera (Fig. 1), and this includes the recently established *Rhodofomes*, occupying a distinct and prominent clade^[4,20,59,60]. *Rhodofomes* clade is closely affiliated with *Brunneoporus malicola* (Berk. & M.A. Curtis) Audet, but exhibits minimal similarity, both morphologically and phylogenetically. Compared to other known species, distinguishing features of *R. flavomarginatus* sp. nov. include dimidiate, solitary, larger, and thicker basidiocarp possessing wide obtuse margin, with capitate basidioles, short basidia (6.2–13.8 × 3.5–5.7 µm) cylindric to ellipsoid basidiospore (5.1–6.0 × 2.7–3.9 µm) (Table 2). The second group features sequences from *Climacocystis*, forming a highly cohesive cluster of white-rotting species. Each of the tree species formed a well-defined clade with high supports. *Climacocystis temperata* sp. nov. is different from the other congeneric species by its larger basidiocarp (up to 19 cm wide) with abundant narrow, multifiform cystidia, with zonate, white upper surface and yellowish pore surface, wide-pored 1–3 (usually

2)/mm, with distinctly larger ellipsoid basidiospores (6.7–10.7 × 3.9–6.1 µm). These morphological and phylogenetic differences provide the basis for proposing a new species.

Daedalea dickinsii, *Neoantrodia serialis*, and *Rhodofomes roseus* were new records added to the country's polypore inventory. After the species identifications based on phylogenetic assessments, morphological characters were examined to confirm the identities. The examined *Daedalea dickinsii* morphologically corresponds to the original description by Yasuda^[60]. Further, our collected specimen of *R. roseus* exhibited morphological and phylogenetic similarities with the description provided by Gilbertson & Ryvarden^[17], Han et al.^[61], and Justo et al.^[8], corroborated the initial proposal made by Kotlaba & Pouzar^[62]. Similarly, *Neoantrodia serialis* in Pakistan demonstrates noteworthy morphological similarity to available species descriptions. *Neoantrodia serialis* was originally identified as *Anurodia serialis* (Fr.) by Donk in 1966^[63]. Later, phylogenetic reconfiguration of *Anurodia* s.l. has resulted in the establishment of multiple novel genera^[6]. Among them, there is *Neoantrodia* Audet, designated for *A. searilis* and its related taxa (approx. 13 species)^[22], which includes the studied species *N. serialis*.

Conclusions

Wood-rot fungal genera are well-studied in various countries, mainly from North America, Europe, and East Asia. However, despite these extensive efforts, significant unaccounted diversity still exists, particularly in several Asian countries, including Pakistan. Consequently, there is a critical need to identify species within these underreported genera, employing diverse taxonomic approaches incorporating molecular, ecological, and morphological evidence. The current study, therefore, aimed to rigorously examine collections based on morphological characteristics and phylogenetic evaluations. In conclusion, the rich biodiversity in the Hindu Kush region offers a favorable habitat for wood-inhabiting fungal species. The numerous collections from the Northern area of Pakistan deserve comprehensive morphoanatomical analysis and molecular investigation. Utilizing such taxonomic data is primarily essential for conservation efforts, resource management, and scientific research not only within the country but also on a global scale. Furthermore, the presence of wood-decaying fungi showcases the region's remarkable ecological and economic significance and contributes to our understanding of global fungal biodiversity.

Author contributions

The authors confirm contribution to the paper as follows: study conception and design: Hussain S, Lim YW, Nisar M; data collection: Hussain S, Ahmad W, Nisar M; analysis and interpretation of results: Hussain S, Cho Y, Ahmad W, Nisar M; draft manuscript preparation: Hussain S, Sher H, Lim YW, Jan T. All authors reviewed the results and approved the final version of the manuscript.

Data availability

The authors of the manuscript confirm that data supporting our study findings are available in the article. Data regarding

Table 2. Morphoanatomical comparisons of the new *Climacocystis* and *Rhodofomes* species and their relatives.

| Species | Genus | | Rhodofomes | | | | Climacocystis | | |
|----------------------------------|---|----------------------------------|--|---------------------------------|----------------------------------|--|--|----------------------------------|--|
| | <i>R. flavomar ginatus</i> ¹ | <i>R. roseus</i> ² | <i>R. incarnates</i> ³ | <i>R. subfeei</i> ⁴ | <i>R. cajanderi</i> ⁵ | <i>C. montana</i> ⁶ | <i>C. borealis</i> ⁷ | <i>C. temperata</i> ¹ | |
| Basidiocarp shape | Ungulate | Dimidiate | Dimidiate | Applanate to triquetrous | Applanate, broadly convex | applanate to dimidiate | Applanate to dimidiate | Applanate to dimidiate | |
| Basidiocarp dim. (L × W × T) cm. | 14 × 10 × 20 | nil × 5–10 × 3–8 | 13 × 6 × 7 | 4 × 10.6 × 2.5 | nil × 3–10 × 10 | 7 × 14 × 2 | 11 × 12 × 3 | 12 × 19 × 3.5 | |
| Margin | Obtuse | Acute to rounded | Acute | Obtuse to acute | Acute | NA | acute | Entire to serrate | |
| Growth habit | Solitary | imbricate | NA | Single or imbricate | Imbricate | Imbricate | Imbricate | imbricate | |
| Pileal surface color | Dark grayish brown | Brownish black | Brownish gray to grayish black | cinnamon brown to fawn brown | Pink to grey, brown, or black | White to pale cream | White to cream | Whitish or pale | |
| Surface texture | Glabrous | NA | Glabrous, finely velvety | Glabrous, rough, | finely velvety or hairy | Tomentose to hirsute | Tomentose to hirsute | Tomentose | |
| Marking or zonation | Azonate, sulcate | Zonate, sulcate | Sulcate | sulcate | Faintly zonate | Azonate | Azonate | Zonate | |
| Pore surface color | Pinkish white | Pink | Pinkish white | Pink to brownish vinaceous | Rosy pink | White to cream | White to cream | Pale yellow | |
| No. pores (mm ⁻¹) | 5–6 (5) | 3–5 | 6–8 | 4–6 | 3/4–5 | 1–3 | 1–3 | 1–3(2) | |
| Hyphal structure | Dimitic | Trimitic | Trimitic | Trimitic | Trimitic | Monomitic | Monomitic | Monomitic | |
| Cont. GH (µm) | 2.6–3.9 | NA | 2.3–3 | 2–3 | NA | 5–8 | 3–7 | 4.7–11.4 | |
| Tramal GH (µm) | 2.3–3.6 | NA | NA | NA | NA | 3–4 | 2.5–4 | 3.9–7.2 | |
| Cystidia | Absent | NA | NA | NA | NA | Ventricose, without crystals, 35–60 µm | Ventricose, with apical crystals, 30–50 µm | Varied in shape, 22.8–58 µm | |
| Cystidioles | Club shaped | Absent | Subulate | Fusoid | Subfusiform or irregular | Absent | Absent | Absent | |
| Basidial sterigma | 4–sterigmate | 4–sterigmate | 2–sterigmate | 4–sterigmate | 4–sterigmate | 4–sterigmate | 4–sterigmate | 4–sterigmate | |
| Basidia dim. (µm) | 6.2–13.8 × 3.5–5.7 | 10–18 × 4–6 | 15–19 × 4–6.3 | 9–18 × 4–6 | 10–12 × 3–4 | 20–27 × 6–7 | 25–30 × 6–8 | 21.5–47.6 × 5.4–8.2 | |
| Basidiospore shape | Cylindric to ellipsoid | Subcylindrical to slightly ovoid | Ellipsoid, frequently curved | Cylindrical to oblong-ellipsoid | Allantoid | Ellipsoid to subcylindrical | Ellipsoid to subcylindrical | Ellipsoid to subcylindrical | |
| Basidiospores length (µm) | 5.1–6.0 × 2.7–3.9 | 5.5–7.5 × 2–2.5 | 4.5–6.3 × 2.2–2.9 | 4–5 × 1.9–2.4 | 5–7 × 2–3 | 6–8.8 × 3–4.2 | 5–6.8 × 3.2–4 | 6.7–10.7 × 3.9–6.1 | |
| Q range | 1.7–2.0 | NA | NA | 2.05–2.1 | NA | 1.85–1.89 | 1.6–1.67 | 1.40–1.51 | |
| Host plant | <i>Abies pindrow</i> | <i>Picea abies</i> | <i>Fraxinus mandshurica</i> , <i>Pinus</i> sp. | <i>Cunninghamia lanceolata</i> | <i>Pinus</i> spp. | <i>Picea</i> spp. | <i>Pinus</i> spp., <i>Picea</i> spp. | <i>Abies pindrow</i> | |

Species references: 1. This study; 2. Carranza-Morse & Gilbertson^[64]; Gilbertson & Ryvarden^[17]; Han et al.^[5]; Justo et al.^[8]; 3. Kim et al.^[59]; 4. Han & Cui^[21]; 5. Justo et al.^[8]; 6. Song et al.^[11]; 7. Gilbertson & Ryvarden^[17]; Nuñez & Ryvarden^[13]; Dal^[14]; Song et al.^[11]; * NA = Not available.

species/specimen DNA sequences are publically available on the accession provided in Table 1, in the GenBank data base of NCBI.

Acknowledgments

We gratefully acknowledge the support of the laboratories: Molecular Ecophylogeny, School of Biological Sciences, and Institute of Microbiology, Seoul National University, South Korea, and the Department of Botany, University of Malakand, KP, Pakistan. Their assistance was vital in conducting this study.

Conflict of interest

The authors declare that they have no conflict of interest.

Dates

Received 20 October 2023; Revised 21 March 2024; Accepted 3 April 2024; Published online 29 April 2024

References

- Runnel K, Miettinen O, Lohmus A. 2021. Polypore fungi as a flagship group to indicate changes in biodiversity – a test case from Estonia. *IMA Fungus* 12:2
- Moose RA, Schigel D, Kirby LJ, Shumskaya M. 2019. Dead wood fungi in North America: an insight into research and conservation potential. *Nature Conservation* 7(32):1–7
- Liu S, Zhou JL, Song J, Sun YF, Dai YC, et al. 2023. Climacocystaceae fam. nov. and Gloeoporellaceae fam. nov., two new families of Polyporales (Basidiomycota). *Frontiers in Microbiology* 14:1115761
- Ortiz-Santana B, Lindner DL, Miettinen O, Justo A, Hibbett DS. 2013. A phylogenetic overview of the antrodia clade (Basidiomycota, Polyporales). *Mycologia* 105:1391–1411
- Han ML, Chen YY, Shen LL, Song J, Vlasák J, et al. 2016. Taxonomy and phylogeny of the brown-rot fungi: *Fomitopsis* and its related genera. *Fungal Diversity* 80:343–373
- Audet S. 2017. New genera and new combinations in *Antrodia* sl. *Mushrooms Nomenclatural Novelties*. pp. 1–9. <https://sergeaudetmyco.com/antrodia/>
- Binder M, Justo A, Riley R, Salamov A, Lopez-Giraldez F, et al. 2013. Phylogenetic and phylogenomic overview of the Polyporales. *Mycologia* 105:1350–73
- Justo A, Miettinen O, Floudas D, Ortiz-Santana B, Sjökvist E, et al. 2017. A revised family-level classification of the Polyporales (Basidiomycota). *Fungal Biology* 121:798–824
- Liu S, Song CG, Xu TM, Ji X, Wu DM, et al. 2022. Species diversity, molecular phylogeny, and ecological habits of *Fomitopsis* (Polyporales, Basidiomycota). *Frontiers in Microbiology* 13:859411
- Kotlíba F, Pouzar Z. 1958. Polypori novi vel minus cogniti Cechoslovakiae III. *Ceská Mykologie* 12:95–104
- Song J, Chen YY, Cui BK. 2014. Phylogeny and taxonomy of *Climacocystis* (Polyporales) in China. *Cryptogamie, Mycologie* 35(3):221–31
- Ryvarden L, Gilbertson RL. 1993. *European Polypores, Part 1: Synopsis Fungorum* 6. Norway: Fungiflora, Oslo. pp. 1–387.
- Núñez M, Ryvarden L. 2001. *East Asian polypores 2: Synopsis Fungorum* 14: 165e522. Norway: Fungiflora, Oslo. pp. 1–280.
- Dai YC. 2012. Polypore diversity in China with an annotated checklist of Chinese polypores. *Mycoscience* 53:49–80
- Miettinen O, Larsson E, Sjökvist E, Larsson KH. 2012. Comprehensive taxon sampling reveals unaccounted diversity and morphological plasticity in a group of dimitic polypores (Polyporales, Basidiomycota). *Cladistics* 28:251–70
- Ryvarden L, Johansen I. 1980. *A preliminary polypore flora of East Africa*. Fungiflora, Oslo, Norway. 636 pp.
- Gilbertson RL, Ryvarden L. 1986. *North American Polypores 1: Abortiporus – Lindtneria*. Norway: Fungiflora, Oslo. pp. 1–433.
- Hattori T, Sotome K. 2013. Type studies of the polypores described by E.J.H. Corner from Asia and West Pacific areas VIII. Species described in *Trametes* (2). *Mycoscience* 54:297–308
- Li HJ, Han ML, Cui BK. 2013. Two new *Fomitopsis* species from southern China based on morphological and molecular characters. *Mycological Progress* 12:709–18
- Han ML, Song J, Cui BK. 2014. Morphology and molecular phylogeny for two new species of *Fomitopsis* (Basidiomycota) from South China. *Mycological Progress* 13:905–14
- Han ML, Cui BK. 2015. Morphological characters and molecular data reveal a new species of *Fomitopsis* (Polyporales) from southern China. *Mycoscience* 56(2):168–176
- Soares AM, Nogueira-Melo G, Plautz HL Jr, Gibertoni TB. 2017. A new species, two new combinations and notes on *Fomitopsis*-*daceae* (Agaricomycetes, Polyporales). *Phytotaxa* 331:75–83
- Haight JE, Laursen GA, Glaeser JA, Taylor DL. 2016. Phylogeny of *Fomitopsis pinicola*: a species complex. *Mycologia* 108:925–38
- Haight JE, Nakasone KK, Laursen GA, Redhead SA, Taylor DL, et al. 2019. *Fomitopsis mounceae* and *F. schrenkii*—two new species from North America in the *F. pinicola* complex. *Mycologia* 111:339–57
- Liu S, Song CG, Cui BK. 2019. Morphological characters and molecular data reveal three new species of *Fomitopsis* (Basidiomycota). *Mycological Progress* 18:1317–27
- Liu S, Han ML, Xu TM, Wang Y, Wu DM, et al. 2021. Taxonomy and phylogeny of the *Fomitopsis pinicola* complex with descriptions of six new species from east Asia. *Frontiers in Microbiology* 12:644979
- Zhou M, Wang CG, Wu YD, Liu S, Yuan Y. 2021. Two new brown rot polypores from tropical China. *Mycoskeys* 82:173–97
- Binder M, Hibbett DS, Larsson KH, Larsson E, Langer E, et al. 2005. The phylogenetic distribution of resupinate forms across the major clades of mushroom-forming fungi (Homobasidiomycetes). *Systematics and Biodiversity* 3:113–57
- Ali K, Khan N, Rahman IU, Ahmad H, Jury S. 2015. Multivariate analysis and vegetation mapping of a biodiversity hotspot in the Hindu Kush Mountains. *International Journal of Advanced Research* 3(6):990–1006
- Razaq A, Shahzad S. 2017. Additions to the diversity of mushrooms in Gilgit-Baltistan, Pakistan. *Pakistan Journal of Botany* 49:305–9
- Aman N, Khalid AN, Moncalvo JM. 2022. A compendium of macrofungi of Pakistan by ecoregions. *Mycoskeys* 89:171–233
- Petersen JH. 1996. *Farvekort. The Danish mycological society's colour-chart*. Greve, Denmark: Foreningen til Svampekundskabens Fremme. pp. 1–6.
- Hu Y, Karunarathna SC, Li H, Galappaththi MCA, Zhao CL, et al. 2022. The impact of drying temperature on basidiospore size. *Diversity* 14:239
- Ji X, Zhou JL, Song CG, Xu TM, Wu DM, et al. 2022. Taxonomy, phylogeny and divergence times of *Polyporus* (Basidiomycota) and related genera. *Mycosphere* 13:1–52
- Banik MT, Lindner DL, Ortiz-Santana B, Lodge DJ. 2012. A new species of *Laetiporus* (Basidiomycota, Polyporales) from the Caribbean basin. *Kurtziana* 37:15–21
- Tsujikawa K, Kanamori T, Iwata Y, Ohmae Y, Sugita R, et al. 2003. Morphological and chemical analysis of magic mushrooms in Japan. *Forensic Science International* 138:85–90
- Murray MG, Thompson WF. 1980. Rapid isolation of high molecular weight plant DNA. *Nucleic Acids Research* 8:4321–26
- Stirling D. 2003. DNA extraction from fungi, yeast, and bacteria. In *PCR Protocols: Methods in Molecular Biology*, eds. Bartlett JMS, Stirling D. vol. 226. Totowa, New Jersey: Humana Press. pp. 53–54. <https://doi.org/10.1385/1-59259-384-4:53>

39. Gardes M, Bruns TD. 1993. ITS primers with enhanced specificity for basidiomycetes-application to the identification of mycorrhizae and rusts. *Molecular Ecology* 2:113–118
40. White TJ, Bruns T, Lee S, Taylor J. 1990. Amplification and direct sequencing of fungal ribosomal RNA genes for phylogenetics. In *PCR protocols: a guide to methods and applications*, eds. Innis MA, Gelfand DH, Sninsky JJ, White TJ. New York: Academic Press. pp. 315–22. <https://doi.org/10.1016/B978-0-12-372180-8.50042-1>
41. Vilgalys R, Hester M. 1990. Rapid genetic identification and mapping of enzymatically amplified ribosomal DNA from several *Cryptococcus* species. *Journal of Bacteriology* 172:4238–46
42. Schoch CL, Seifert KA, Huhndorf S, Robert V, Spouge JL, et al. 2012. Nuclear ribosomal internal transcribed spacer (ITS) region as a universal DNA barcode marker for *Fungi*. *Proceedings of the National Academy of Sciences*, 109:6241–46
43. Altschul SF, Gish W, Miller W, Myers EW, Lipman DJ. 1990. Basic local alignment search tool. *Journal of Molecular Biology* 215:403–10
44. Karsch-Mizrachi I, Takagi T, Cochrane G. 2018. The international nucleotide sequence database collaboration. *Nucleic Acids Research* 46:D48–D51
45. Nilsson RH, Tedersoo L, Abarenkov K, Ryberg M, Kristiansson E, et al. 2012. Five simple guidelines for establishing basic authenticity and reliability of newly generated fungal ITS sequences. *Mycologia* 4:37–63
46. Schoch CL, Robbertse B, Robert V, Vu D, Cardinali G, et al. 2014. Finding needles in haystacks: linking scientific names, reference specimens and molecular data for *Fungi*. *Database* 2014:bau061
47. Katoh K, Rozewicki J, Yamada KD. 2019. MAFFT online service: multiple sequence alignment, interactive sequence choice and visualization. *Briefings in Bioinformatics* 20:1160–66
48. Hall T. 2011. BioEdit: an important software for molecular biology. *GERF Bulletin of Biosciences* 2:60–61
49. Shen Q, Geiser DM, Royse DJ. 2002. Molecular phylogenetic analysis of *Grifola frondosa* (maitake) reveals a species partition separating eastern North American and Asian isolates. *Mycologia* 94:472–82
50. Shen LL, Wang M, Zhou JL, Xing JH, Cui BK, et al. 2019. Taxonomy and phylogeny of *Postia*. Multi-gene phylogeny and taxonomy of the brown-rot fungi: *Postia* (Polyporales, Basidiomycota) and related genera. *Persoonia - Molecular Phylogeny and Evolution of Fungi* 42:101–26
51. Nguyen LT, Schmidt HA, Von Haeseler A, Minh BQ. 2015. IQ-TREE: a fast and effective stochastic algorithm for estimating maximum-likelihood phylogenies. *Molecular Biology and Evolution* 32:268–74
52. Darriba D, Taboada GL, Doallo R, Posada D. 2012. jModelTest 2: more models, new heuristics and parallel computing. *Nature Methods* 9:772
53. Hoang DT, Chernomor O, Von Haeseler A, Minh BQ, Vinh LS. 2018. UFBoot2: improving the ultrafast bootstrap approximation. *Molecular Biology and Evolution* 35:518–22
54. Ronquist F, Huelsenbeck JP. 2003. MrBayes 3: Bayesian phylogenetic inference under mixed models. *Bioinformatics* 19:1572–74
55. Lindner DL, Banik MT. 2008. Molecular phylogeny of *Laetiporus* and other brown rot polypore genera in North America. *Mycologia* 100:417–30
56. Li HJ, Cui BK. 2013. Two new *Daedalea* species (Polyporales, Basidiomycota) from South China. *Mycoscience* 54:62–68
57. Cristaldo Centurión E, Kossmann T, Campi M, Maubet Y, Costa-Rezende D, et al. 2022. Neotropical *Daedalea* (Basidiomycota, Fomitopsidaceae) revisited: *Daedalea rajchenbergiana* sp. nov. from Brazil. *Lilola* 59:273–89
58. Decock CA, Ryvarden L, Amalfi M. 2022. *Niveoporofomes* (Basidiomycota, Fomitopsidaceae) in Tropical Africa: two additions from Afromontane forests, *Niveoporofomes oboensis* sp. nov. and *N. widdringtoniae* comb. nov. and *N. globosporus* comb. nov. from the Neotropics. *Mycological Progress* 21:29
59. Kim KM, Lee JS, Jung HS. 2007. *Fomitopsis incarnatus* sp. nov. based on generic evaluation of *Fomitopsis* and *Rhodofomes*. *Mycologia* 99:833–41
60. Yasuda A. 1922. Notes on *Fungi*. *The Botanical Magazine*. 36:128
61. Han ML, Vlasak J, Cui BK. 2015. *Daedalea americana* sp. nov. (Polyporales, Basidiomycota) evidenced by morphological characters and phylogenetic analysis. *Phytotaxa* 204:277–86
62. Kotlaba F, Pouzar Z. 1990. Type studies of polypores described by A. Pilát-III. *Type studies of polypores described by A. Pilát-III*. 44:228–37
63. Donk MA. 1966. Notes on European polypores-I. *Persoonia-Molecular Phylogeny and Evolution of Fungi* 4:337–43
64. Carranza-Morse J, Gilbertson RL. 1986. Taxonomy of the *Fomitopsis rosea* complex (Aphyllphorales; Polyporaceae). *Mycotaxon* 25:469–86



Copyright: © 2024 by the author(s). Published by Maximum Academic Press, Fayetteville, GA. This article is an open access article distributed under Creative Commons Attribution License (CC BY 4.0), visit <https://creativecommons.org/licenses/by/4.0/>.